Modelling of Neutrosophic Set-Based k-Nearest Neighbors Classifier for Virus Pneumonia and COVID-19 Recognition

Imène Issaoui[1,*], Afef Selmi[2]

[1]Unit of Scientific Research, Applied College, Qassim University, Buraydah, Saudi Arabia.
[2]Department of Information Technology, College of Computer, Qassim University, Buraydah, Saudi Arabia
Emails: i.issaoui@qu.edu.sa; a.selmi@qu.edu.sa

Abstract

COVID19 otherwise called Severe Acute Respiratory Syndrome Corona virus-2 is an infectious illness. Another transmittable infection called Pneumonia is mainly attributable to infection because of bacteria in the alveoli of the lungs. Once a diseased lung tissue has infection, it elevates excretion in it. Specialists conduct health examinations and identify the patient through ultrasound, biopsy, or Chest X-ray of lungs to identify whether the patient has these diseases. Incorrect treatment, misdiagnosis, and if the disease was disregarded will result in the fatality. The development of Deep Learning and neutrosophic set (NS) supports the decision-making procedure of professionals to identify patients with this disease. NS is a prolongation of the fuzzy set and classical theories. The NS determines three memberships such as T, I and F. T, I, and F display the degree of truth, the false, and the indeterminacy membership, correspondingly. This enables a more nuanced representation of contradiction, uncertainty, and ambiguity within the dataset, allowing superior handling of imprecise and complex data. This study develops a new Deep learning with Neutrosophic Set-Based k-Nearest Neighbors Classifier for disease detection (DLNSKNN-DD) technique. The major purpose of the DLNSKNN-DD method is to identify the existence of virus pneumonia and COVID-19. In the DLNSKNN-DD technique, the feature extraction from the medical images is carried out by residual network (ResNet50v2). Moreover, the parameter tuning of the ResNetv2 model is done using Adadelta optimizer. The DLNSKNN-DD technique exploits NSKNN model for classification purposes. The performance evaluation of the DLNSKNN-DD algorithm can be assessed on medicinal image dataset. The experimental outcomes underlined the effectual recognition results of the DLNSKNN-DD technique on the identification of diseases

Keywords: Virus Pneumonia; Sars-Cov-2; COVID-19 diagnosis; Machine Learning; Neutrosophic Logic; Neutrosophic Soft Set

1. Introduction

Numerous uncertainty issues can be met in several regions of our everyday life, like physics and engineering [1]. Due to this intention, conveying uncertainty issues in the precise method and gaining the precise outcome in resolving the issue are the dual significant features of achieving the finest decision-making procedure [2]. Many researchers have got numerous dissimilar mathematical methods to the survey, which can transport this procedure to the precise outcome [3]. While, fuzzy sets are projected by Zadeh, which is the initial numerical technique put onward in this field, it is an effective model [4]. In present scenario, numerous mathematical techniques like neutrosophic set (NS), interval-valued intuitionistic FS, picture fuzzy set, Pythagorean fuzzy set, single-valued NS, hypersoft set, and fermatean fuzzy sets, which are dissimilar additions of this model, are put onward [5].

COVID19 and human coronaviruses are categorized under the family of Coronaviridae. If these infections affect individuals, then it affects Severe Acute Respiratory Syndrome (SARS), or moderate cold Middle East Respiratory Syndrome (MERS) [6]. Where, the SARS is a virus-related lung illness affected by SARS-associated coronavirus (SARS-CoV) [7] [8]. The NAT is employed to identify accurate nucleic acid systems and types of organisms, mostly bacteria that cause illness in blood, urine or tissue [9]. While, the NAT and recognition tools play significant

DOI: https://doi.org/10.54216/IJNS.250105
Received: February 01, 2024 Revised: April 02, 2024 Accepted: June 21, 2024

parts in classifying CT scans, COVID19, and X-ray imageries, which are effective and real techniques for identifying the seriousness of lung infection estimated to be interrelated with COVID19 [10].

DL and ML are sub-types of AI, which are measured in mechanizing the procedure of COVID19 recognition over the identification of the chest X-ray/CT scan imageries [11]. An analysis of the work displays that DL-based methods attempting this kind of identification issue exceeded ML-based techniques [12]. Great identification performance of recall, accuracy, F1-measure and precision was stated in many research works [13]. On the other hand, many classification techniques were tested and trained on lesser datasets (recognized to the lack of COVID19 patient information later above one year, then this virus in progress) including either dual (COVID19 ill vs. ordinary) or 3 classes (COVID19 ill, pneumonia case, ordinary) [14]. This size of dataset restraint creates the projected methods, which is a proof of theory of COVID19 patient recognition, and so these methods need re-assessment with greater datasets [15].

This study develops a new Deep learning with Neutrosophic Set-Based k-Nearest Neighbors Classifier for disease detection (DLNSKNN-DD) method. The objective of the DLNSKNN-DD method is to detect the presence of virus pneumonia and COVID-19. In the DLNSKNN-DD technique, the feature extraction from the medical images is carried out by residual network (ResNet50v2). Moreover, the parameter tuning of the ResNetv2 model is done using Adadelta optimizer. For classification purposes, the DLNSKNN-DD technique exploits NSKNN model. The performance evaluation of the DLNSKNN-DD technique can be assessed on medical image dataset.

2. Related Works

In [16], five diverse deep learning (DL) methods namely ResNet34, InceptionResNetV2, InceptionV3, ResNet18, DenseNet161, and their combination utilizing majority voting are employed for classification by implementing chest X-ray images. Multiclass classification was achieved by anticipating several pathologies for every patient. Initially, every network's interpretability is examined by utilizing local techniques such as input X, occlusion, integrated gradients, saliency, DeepLIFT, BP, and the global model. Althaqafi et al. [17] propose a SCO with DL-based disease recognition and organization (SCODL-DDC) approach. This method investigates the CXR images to recognize and categorize the COVID19. Specifically, the proposed model employs the EfficientNet method for the generation of feature vector, and its parameters are altered through the SCO model. Moreover, the QNN method is implemented for the precise classification of COVID19. Lastly, the equilibrium optimizer (EO) model is utilized for optimal hyperparameter selection of the QNN method.

In [18], an image-based recognition of COVID19 employing deep learning (DL) technique is proposed. This paper utilizes chest X-ray images that is predominantly available in most medical facilities. This article applied a CNN technique and pretrained deep neural approaches namely DenseNet121, VGG19, resnet50, and VGG16 for classifying COVID19. Islam et al. [19] present an enhanced DCNN model for detecting and classifying COVID19 employing X-ray and CT images. The pre-processing techniques namely classification variable encoding, filtering, data augmentation, and data normalization are employed before the training stage in combination with the presented technique to enhance the efficiency of the recognition and classification procedures. Also, deep CNN model is implemented for extracting significant factors.

In [20], the mother optimization algorithm with deep learning-based detection and classification (MOA-DLEDC) model is introduced. In this approach, the adaptive median filtering (AMF) method is utilized for removing the noise. Additionally, the intrinsic and complex features are extracted from the DenseNet method. Furthermore, the hyperparameter optimization is achieved by employing MOA. Moreover, the MOA-DLEDC model uses SAE approach for COVID-19 recognition procedure. In [21], a COVID19 recognition model is proposed. Initially, the input images are passed onto the preprocessing process as an input, in order to extract the deep and texture factors. Specifically, the deep features are extracted by utilizing InceptionV3. Later, the extraction of the Local Binary Pattern (LBP) and Local Vector Patterns (LVP) factors is achieved. Furthermore, the extracted factors are given to the presented ensemble classification stage. Also, a Self Adaptive Kill Herd Optimization (SAKHO) model is employed.

3. Materials and Methods

In this study, we have designed a new DLNSKNN-DD method. The objective of the DLNSKNN-DD technique is to detect the presence of virus pneumonia and COVID-19. It contains three distinct kinds of processes involving selection, optimization, and classification processes are shown in Fig. 1.

A. Dataset Details

DOI: https://doi.org/10.54216/IJNS.250105
Received: February 01, 2024 Revised: April 02, 2024 Accepted: June 21, 2024

The performance evaluation of the DLNSKNN-DD technique can be evaluated using CXR dataset [22]. It holds 305 samples with 6 classes as shown in Table 1.

Table 1: Details of dataset

Classes	No. of Images
ARDS	15
COVID-19	220
No Finding	27
Pneumocystis	15
SARS	11
Streptococcus	17
Total Images	305

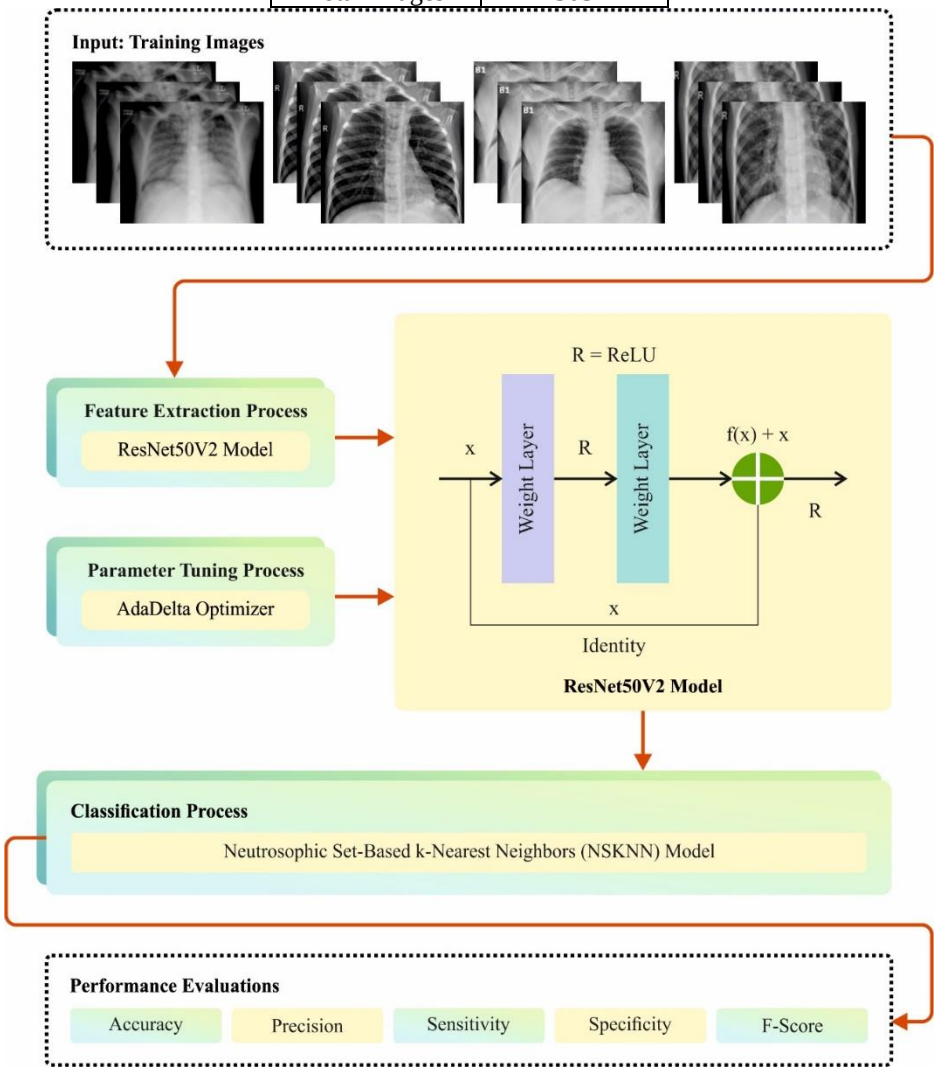

Figure 1: Working flow of DLNSKNN-DD method

B. Model Selection

Initially, the DLNSKNN-DD technique undergoes the extraction of features from the medical images carried out by ResNet50v2. This segment signifies the idea of deep feature extraction and its use in COVID19 recognition [23]. Deep feature extraction requires removing the informative and meaningful aspects from raw data utilizing the DNN model. This feature acquires higher-level representation, which is highly efficient in directing the task.

We used the ResNet50-V2 structure as a deep feature extraction mode for the COVID19 recognition. ResNet50-V2 is nothing but a CNN, which is extremely important in numerous CV tasks. It is a variation of ResNet structure and utilizes skip connection in order to tackle the degradation issue in deep networks. ResNet50-V2 includes 50 layers, and it is pretrained on the dataset of larger-scale images like ImageNet. It uses residual blocks, permitting

DOI: https://doi.org/10.54216/IJNS.250105
Received: February 01, 2024 Revised: April 02, 2024 Accepted: June 21, 2024

the system to discover lasting mapping and aiding the training of methods. Besides, the skip connection permits gradients to flow absolutely from initial to advanced layers, increasing the training procedure. Fig. 2 depicts the architecture of ResNet50v2 model.

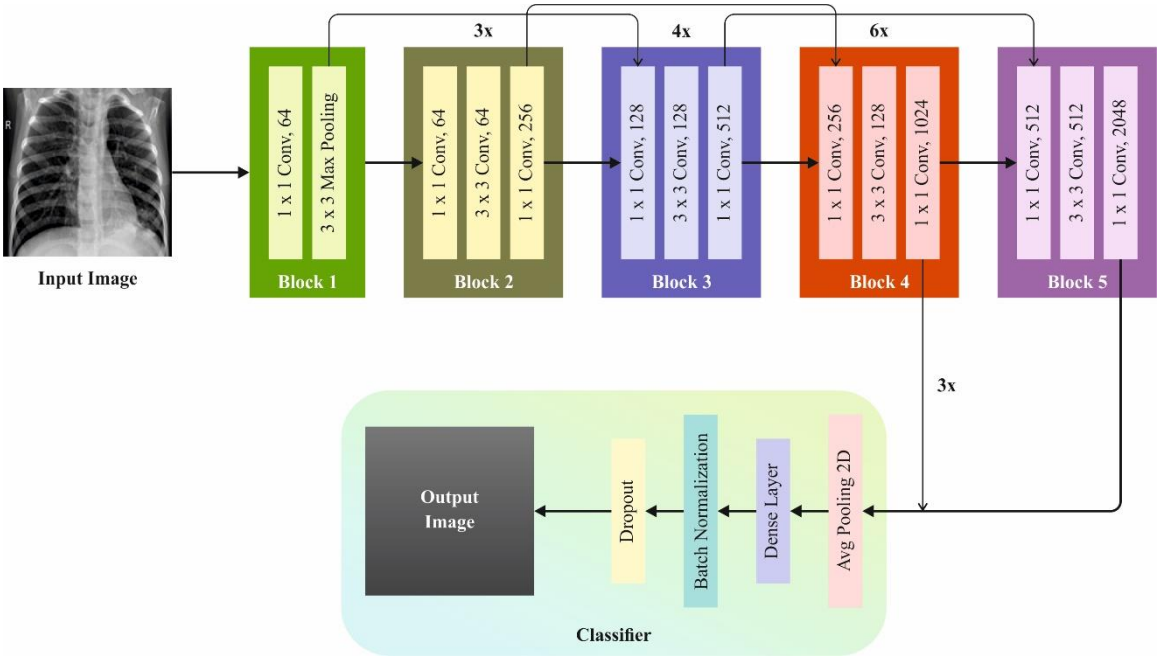

Figure 2: Architecture of ResNet50v2

The ResNet50-V2 structure is helpful for feature extractors in recognition of COVID19 since it obtains hierarchical and complex models from imageries of COVID19. With its deep layer, ResNet50-V2 discovers abstract representations of forms, structures and textures, which is critical in recognizing malignant and benign breast tissues. Influencing the pre-trained ResNet50-V2 method offers the benefit of TL, which contains previously discovered general features from a larger-scale imagery dataset such as ImageNet. The pretraining permits ResNet50-V2 to acquire common image representation, which can be perfected for recognition of COVID19. By using the acquired features from ResNet50-V2, we can recover the performance and precision of COVID19 recognition method.

The features obtained from ResNet50-V2 are achieved as the highest-level representations of input COVID19 imageries, acquiring critical data for recognition and classification tasks. These features are inputs for numerous ML techniques, aiding us to influence the great representation acquired by ResNet50-V2. By leading that act, we aim to optimize the outcomes of COVID19 recognition method. The higher-level feature acquired by ResNet50-V2 delivers a complete and useful representation of the input dataset, refining our skill to discriminate among malignant and benign breast tissues and finally foremost to effectual recognition of COVID19.

C. Model Optimization

Next, the parameter tuning of the ResNetv2 model is done using Adadelta optimizer. When equated with gradient descent, the upgrade regulation of Adagrad doesn't fit a value fixed for the learning rate are employed to parameter optimizer throughout every iteration [24]. Assume that time t is a specific iteration, the objective function gradient to the parameter is given below:

$$g_{t,i} = \nabla_{\theta} J(\theta_j) \tag{1}$$

Here, θ epitomizes the parameter, J signifies the function of objective and ∇ denotes the derivative sign.

Normal stochastic gradient descent method utilizes a similar rate of learning for every θ_i. So, after repeating at t time, the changing procedure of a θ_i specified parameter vector is given below:

$$\theta_{i+1,i} = \theta_{t,i} - \eta \cdot g_{t,i} \tag{2}$$

$$\Delta\theta_t = -\eta \cdot g_{t,i} \tag{3}$$

Whereas, η denotes the rate of learning, $\Delta\theta_t$ signifies the modification in the θ_i parameter at the t^{th} iterations.

DOI: https://doi.org/10.54216/IJNS.250105
Received: February 01, 2024 Revised: April 02, 2024 Accepted: June 21, 2024

In upgrade regulation of Adagrad, the learning rate will modify with all the iterations as per the past gradient:

$$\theta_{t+1,i} = \theta_{t,i} - \frac{\eta}{\sqrt{G_t + \varepsilon}} \cdot g_{t,i} \tag{4}$$

$$\Delta\theta_t = -\frac{\eta}{\sqrt{G_t + \varepsilon}} \cdot g_{t,i} \tag{5}$$

Whereas, $G^t \in R^{d\times d}$ denotes a matrix of diagonal. ε represents a smooth entry that stops null division.

Adagrad computes the quantity of squares in the denominator since every parameter should be optimistic throughout the training procedure. In this method, in the next stage, the upgrading capability of the system will convert into weaker, and the capability to absorb more data will also turn into weaker since the learning rate becomes much smaller. To resolve these issues, the Adadelta method is developed. The value of dynamic mean is only based on the existing values of gradient and mean of preceding time:

$$E[g^2]_t = \gamma E[g^2]_{t-1} + (1-\gamma) g_t^2 \tag{6}$$

Whereas, γ is like the term of momentum and is near 0.9.

Just by switching the original G_t as $E[g^2]_t$:

$$\Delta\theta_t = -\frac{\eta}{\sqrt{E[g^2]_t + \varepsilon}} \cdot g_{t,i} \tag{7}$$

The denominator is just indicated as RMS, which indicates the error of root mean square:

$$\Delta\theta_t = -\frac{\eta}{RMS[g]_t} \cdot g_t \tag{8}$$

In the upgrade, the mean of exponential decay is explained as a substitute for the gradient squared.

$$E[\Delta\theta_t^2]_t = \gamma E[\Delta\theta_t^2]_{t-1} + (1-\gamma)\Delta\theta_t \tag{9}$$

By swapping $RMS[\Delta\theta]_{t-1}$ for the rate of learning η, the Adadelta upgrade regulation is attained:

$$\theta_{t+1} = \theta_t - \frac{RMS[\Delta\theta]_{t-1}}{RMS[g]_t} \cdot g_t \tag{10}$$

The Adadelta optimizer is used to derive an FF for accomplishing superior classifier outcomes. It describes a positive integer to describe the improved accuracy of the solution candidate. Now, the decay of the classifier error rate is assumed as FF.

$$fitness(x_i) = ClassifierErrorRate(x_i)$$
$$= \frac{No.of\ misclassified\ samples}{Total\ No.of\ samples} * 100 \tag{11}$$

D. Design of NSKNN Classifier

For classification purposes, the DLNSKNN-DD technique exploits NSKNN model. Some basic definitions are discussed in this section consists [25].

Definition1 (Neutrosophic Soft Set (NSS)): Consider $\mathbb{U}$ as a universe and $\mathbb{E}$ as a concerning attributes. Assume $\mathbb{P}(\mathbb{U})$ as a group of neutrosophic values of $\mathbb{U}$ and $\subseteq E$. The pair $(\mathbb{F} = \mathbb{A})$ is known as a NSS over $\mathbb{U}$ in which $\mathbb{F}$ map with $\mathbb{F} =: \mathbb{A} \to \mathbb{P}(\mathbb{U})$.

Definition 2 (HyperSoft Set): consider $\mathbb{U}$ as a universe and $\mathbb{P}(\mathbb{U})$ as the power of $\mathbb{U}$. Assume $1^1, 1^2, 1^3 \dots 1^n$, for $n \geq 1$, as n definite attributes, whose related attribute value is a set $L^1, L^2, L^3 \dots L^n$, correspondingly, with $L^i \cap L^j = \emptyset$, for $i \neq j$ and $i, j \in \{1,2,3 \dots n\}$. The couple $L^1 \times L^2 \times L^3 \dots L^n)$ is Hypersoft set over $\mathbb{U}$ in which $\mathbb{F}$ refers to a map provided as $\mathbb{F} =: L^1 \times L^2 \times L^3 \dots L^n \to \mathbb{P}(\mathbb{U})$.

Definition 3 (Neutrosophic Hypersoft Set (NHSS)): Consider $\mathbb{U}$ and $\mathbb{P}(\mathbb{U})$ as universal and power sets of U. Where $1^1, 1^2, 1^3 \dots 1^n$ for $n \geq 1$ is a n definite attribute, whose related attribute value is a set $L^1, L^2, L^3 \dots L^n$, correspondingly, with $L^i \cap L^j = \emptyset$, for $i \neq j$ and $i, j \in \{1,2,3 \dots n\}$ and the relationship $L^1 \times L^2 \times L^3 \dots L^n = \$$, A couple $(\mathbb{F}\ \$)$ is the NHSS over U where $\mathbb{F}$ refers to a map with $\mathbb{F}: L^1 \times L^2 \times L^3 \dots L^n \to \mathbb{P}(\mathbb{U})$ using $\mathbb{F}(L^1 \times L^2 \times$

DOI: https://doi.org/10.54216/IJNS.250105
Received: February 01, 2024 Revised: April 02, 2024 Accepted: June 21, 2024

$L^3 \dots L^n) = \{< x, T\ (₣(\$)), I\ (₣(\$)), F\ (₣(\$)) >, x \in \mathbb{U}\}$ in which $T, I, F : U \to [0,1]$ and $0 \leq T\ (₣(\$)\ ) + I\ (₣(\$)\ ) + F(₣(\$)) \leq 3$.

Definition 4 (Neutrosophic hyperSoftMatrix (NHSM)): Consider $\mathbb{U} = \{u^1, u^2, \dots u^a\}$ and $\mathbb{P}(\mathbb{U})$ as the universe and power sets of the universal set correspondingly. Assume $\mathbb{L}_1, \mathbb{L}_2, \dots \mathbb{L}_b$ for $b \geq 1$ as b definite features, whose attribute value is the sets $\mathbb{L}_1^a$, $\mathbb{L}_2^b$, $\dots \mathbb{L}_=^z$ with the relationship $\mathbb{L}_1^a \times \mathbb{L}_2^b \times \dots \mathbb{L}_b^z$ whereas $a, b, c, \dots z = 1,2, \dots n$. The NHSS $(\mathbb{L}_1^a \times \mathbb{L}_2^b \times \dots \mathbb{L}_b^z)$ over $\mathbb{U}$ with $\mathbb{F}: (L_1^a \times L_2^b \times \dots \mathbb{L}_b^z) \to \mathbb{P}(\mathbb{U})$ is formulated by $(\mathbb{L}_1^a \times \mathbb{L}_2^b \times \dots \mathbb{L}_\times^z) = \{< u, \mathbb{T}_\ell(u), =_\ell\ (u), \mathbb{F}_\ell(u) >, u \in \mathbb{U}, \ell \in (\mathbb{L}_1^a \times \dots \mathbb{L}_b^z)$ Consider $\mathbb{R}_\ell = (\mathbb{L}_1^a \times \mathbb{L}_2^b \times \dots \mathbb{L}_b^z)$ as the relationship with the characteristic functions represented as $X_{\mathbb{R}_\ell} : (\mathbb{L}_1^a \times \mathbb{L}_2^b \times \dots \mathbb{L}_b^z) \to \mathbb{P}(\mathbb{U})$. Next, it is represented by $X_{\mathbb{R}_\ell} = \{< u, \mathbb{T}_\ell(u), I_\ell(u), \mathbb{F}_\ell(u) > u \in \mathbb{U}, \ell \in (\mathbb{L}_1^a \times \mathbb{L}_2^b \times \dots \mathbb{L}_b^z)\}$ and known as NHSM.

If $A_{ij} = X_{\mathbb{R}=}\left(u^i, \mathbb{L}_j^k\right)$, where $i = 1,2,3 \dots a, j = 1,2,3, \dots b, k = a, b, c, \dots z$, then the matrix can be represented by $[A_{ij}]_{a\times b} = \begin{pmatrix} A_{11} & A_{12} & \dots & A_{1b} \\ A_{21} & A_{22} & \dots & A_{2b} \\ \vdots & \vdots & \ddots & \vdots \\ A_{a1} & A_{a2} & \dots & A_{ab} \end{pmatrix}$ where $A_{ij} = (\mathbb{T}_{\mathbb{L}_j^k}(u_i)$,

$\mathbb{I}_{\mathbb{L}_j^k}(u_i), \mathbb{F}_{\mathbb{L}_j^k}(u_i), u_i \in \mathbb{U}, \mathbb{L}_j^k \in (\mathbb{L}_1^a \times \mathbb{L}_2^b \times \dots \mathbb{L}_b^z)) = (\mathbb{T}_{ijk}^A, \mathbb{I}_{ijk}^A, \mathbb{F}_{ijk}^A)$.

Therefore, NHSS is represented in terms of NHSM. It implies that they are similar. Its general form is represented as $[A_{ij}]_{a\times b}$, at the page bottom.

As classical KNN undergoes allocating equivalent weights to classes in the training data, neutrosophic membership is implemented to conquer these drawbacks [26]. Neutrosophic membership reflects the significance of data points in its class labels and this membership is utilized as a new process for KNN model.

Neutrosophic set can describe a membership sample that belongs to indeterminacy, truth, and false. In a supervised way, an unsupervised neutrosophic clustering model (NCM) is utilized. Crisp clustering method considers that the data point must belong to a cluster based on the proximity to the cluster centre. Fuzzy clustering method allocated fuzzy membership to all the data points based on the propinquity to the cluster center. Neutrosophic clustering allocated T, I, and F memberships to all the data points to the centre of the cluster and center means of two clusters. The cluster center can be evaluated as the label of a training data sample that is well-known in supervised learning. Next, the T, F, and I membership values are defined by the following expression:

$$T_{ij} = \frac{(x_i - c_j)^{-\left(\frac{2}{m-1}\right)}}{\sum_{j=1}^{C}(x_i - c_j)^{-\left(\frac{2}{m-1}\right)} + (x_i - \overline{c}_{imax})^{-\left(\frac{2}{m-1}\right)+\delta^{-\left(\frac{2}{m-1}\right)}}} \tag{12}$$

$$F_i = \frac{(\delta)^{-\left(\frac{2}{m-1}\right)}}{\sum_{j=1}^{C}(x_i - c_j)^{-\left(\frac{2}{m-1}\right)} + (x_i - \overline{c}_{imax})^{-\left(\frac{2}{m-1}\right)+\delta^{-\left(\frac{2}{m-1}\right)}}} \tag{13}$$

$$I_i = \frac{(x_i - \overline{c}_{imax})^{-\left(\frac{2}{m-1}\right)}}{\sum_{j=1}^{C}(x_i - c_j)^{-\left(\frac{2}{m-1}\right)} + (x_i - \overline{c}_{imax})^{-\left(\frac{2}{m-1}\right)+\delta^{-\left(\frac{2}{m-1}\right)}}} \tag{14}$$

Here, c_j is the center of cluster j, m denotes a constant, and δ indicates the normalization parameter. For all the i^{th} points, the $\overline{c}_{imax}$ refers to the mean of both cluster centers in which the T values are higher than the others. T_{ij}, F_i and I_i are the true, false, and indeterminacy membership of i^{th} points. Higher T_{ij} implies that the i^{th} points are near the cluster and unlikely a noise. Greater I_i denotes that the i^{th} points are between both clusters and greater F_i shows that i^{th} points can be a noise. The last membership values for i^{th} points are evaluated.

The membership for indefinite samples χ_u to i^{th} classes after defining the neutrosophic membership triples are evaluated by the following expression:

$$\mu_{ju} = \frac{\Sigma_{i=1}^{k} d_i\left(T_{ij} + I_i - F_i\right)}{\Sigma_{i=1}^{k} d_i} \tag{15}$$

DOI: https://doi.org/10.54216/IJNS.250105
Received: February 01, 2024 Revised: April 02, 2024 Accepted: June 21, 2024

$$d_i = \frac{1}{\|x_u - \chi_i\|^{\frac{2}{q-1}}} \tag{16}$$

Where d_i refers to the distance function to evaluate the distance between x_j and x_u, k denotes the number of kNN and q represents an integer. The neutrosophic k- NN allocates x_u to the class after assigning the neutrosophic membership grade of indefinite samples x_u to the classes. The subsequent step is utilized to construct the NS-k-NN technique:

Initialize the cluster center based on the labeled data and utilize Eqs. (12) to (14) for calculating the, I, and F values for all the training datasets.

Calculate membership grade of test datasets based on the Eqs. (15) and (16).

Allocate classes of the indefinite testing datasets to the classes whose neutrosophic membership is higher.

4. Results Analysis

In this section, the experimental outcomes underlined the effectual recognition outcomes of the DLNSKNN-DD method on the identification of diseases.

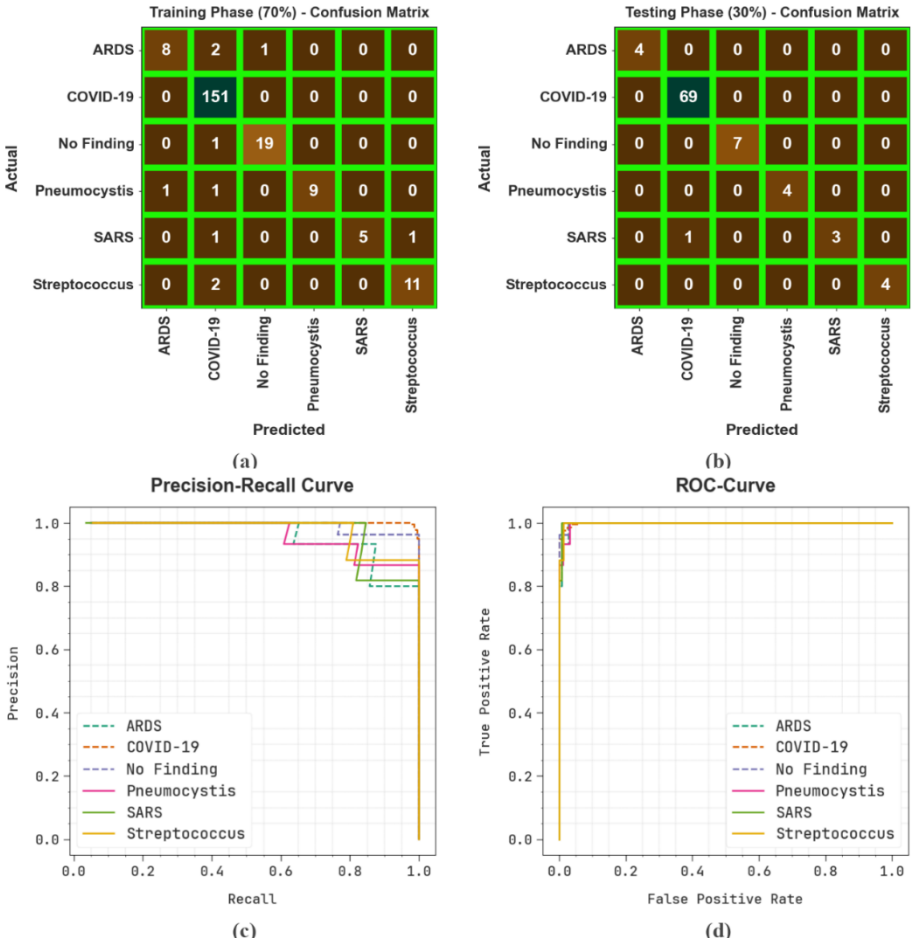

Figure 3: Classifier outcome of (a-b) Confusion matrices and (c-d) PR and ROC curves

Fig. 3 depicts the classifier results of the DLNSKNN-DD system. Figs. 3a-3b describes the confusion matrices presented by the DLNSKNN-DD technique on 70:30 of TRAS/TESS. The figure shows that the DLNSKNN-DD system has known and classified every class exactly. Also, Fig. 3c forms the PR inspection of the DLNSKNN-DD system. The figure is definite that the DLNSKNN-DD methodology has enlarged the highest performance of PR below every class. Lastly, Fig. 3d defines the ROC study of the DLNSKNN-DD method. The figure displays that the DLNSKNN-DD approach has outcome in skilled consequences with the maximum ROC values below different classes.

DOI: https://doi.org/10.54216/IJNS.250105
Received: February 01, 2024 Revised: April 02, 2024 Accepted: June 21, 2024

The pneumonia and COVID19 detection results of the DLNSKNN-DD approach are inspected in Table 2 and Fig. 4. The outcomes appeared that the DLNSKNN-DD model gains improved detection results under all classes. With 70%TRAS, the DLNSKNN-DD technique offers average $accu_y$, $prec_n$, $sens_y$, $spec_y$, and F_{score} of 98.44%, 95.19%, 84.26%, 97.87%, and 89.01%, correspondingly. Additionally, with 730%TESS, the DLNSKNN-DD method offers average $accu_y$, $prec_n$, $sens_y$, $spec_y$, and F_{score} of 99.64%, 99.76%, 95.83%, 99.28%, and 97.50%, correspondingly

Table 2: COVID-19 detection results of DLNSKNN-DD method on 70%TRAS and 30%TESS

Classes	$Accu_y$	$Prec_n$	$Sens_y$	$Spec_y$	F_{score}
TRAS (70%)					
ARDS	98.12	88.89	72.73	99.50	80.00
COVID-19	96.71	95.57	100.00	88.71	97.73
No Finding	99.06	95.00	95.00	99.48	95.00
Pneumocystis	99.06	100.00	81.82	100.00	90.00
SARS	99.06	100.00	71.43	100.00	83.33
Streptococcus	98.59	91.67	84.62	99.50	88.00
Average	98.44	95.19	84.26	97.87	89.01
TESS (30%)					
ARDS	100.00	100.00	100.00	100.00	100.00
COVID-19	98.91	98.57	100.00	95.65	99.28
No Finding	100.00	100.00	100.00	100.00	100.00
Pneumocystis	100.00	100.00	100.00	100.00	100.00
SARS	98.91	100.00	75.00	100.00	85.71
Streptococcus	100.00	100.00	100.00	100.00	100.00
Average	99.64	99.76	95.83	99.28	97.50

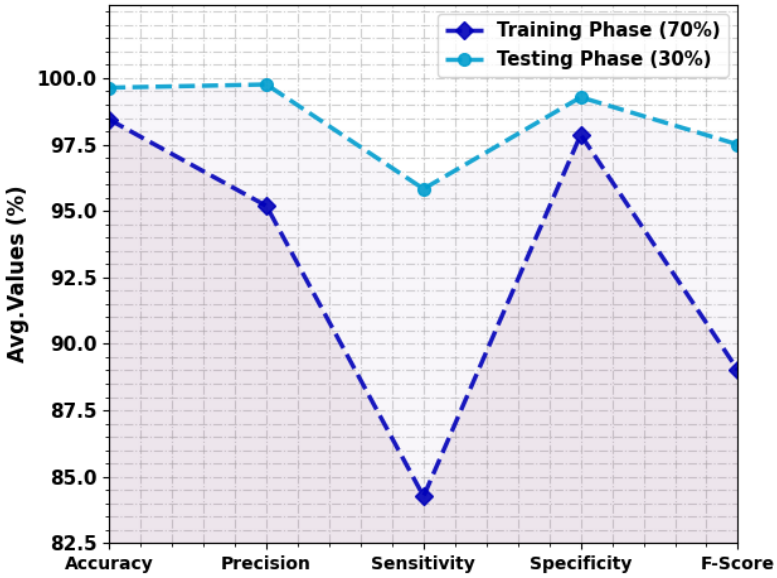

Figure 4: Average values of DLNSKNN-DD technique under 70%TRAS and 30%TESS

In Table 3 and Fig. 5, a detailed comparison study of the DLNSKNN-DD technique with current models is given [17]. The outcomes implied the improved efficacy of the DLNSKNN-DD method in terms of diverse metrics. Based on $accu_y$, the DLNSKNN-DD technique gains increased $accu_y$ of 99.64% while the SCODL-DDC, fusion, InceptionV3, ResNet50, VGG16, and AD-TLCNN models obtain decreased $accu_y$ of 99.45%, 98.97%, 97.65%, 97.08%, 96.59%, 95.07%, and 94.71%, correspondingly. Also, based on $sens_y$, the DLNSKNN-DD technique gains increased $sens_y$ of 95.83% where the SCODL-DDC, fusion, Inceptionv3, ResNet-50, VGG-16, and AD-TLCNN models obtain decreased $accu_y$ of 94.65%, 92.86%, 94.26%, 88.17%, 86.57%, 94.46%, and 93.59%, correspondingly. Besides, based on $spec_y$, the DLNSKNN-DD technique gains increased $accu_y$ of 99.28% while the SCODL-DDC, fusion, InceptionV3, ResNet50, VGG16, and AD-TLCNN models obtain decreased $accu_y$ of 99.11%, 98.45%, 97.68%, 97.85%, 97.80%, 97.18%, and 94.77%, correspondingly. Moreover, based on f_{score}, the DLNSKNN-DD technique gains increased $accu_y$ of 97.50% while the SCODL-DDC, fusion, InceptionV3,

DOI: https://doi.org/10.54216/IJNS.250105
Received: February 01, 2024 Revised: April 02, 2024 Accepted: June 21, 2024

ResNet50, VGG16, and AD-TLCNN models obtain decreased $accu_y$ of 97.27%, 93.16%, 90.43%, 84.07%, 83.26%, 92.33%, and 93.60%, correspondingly.

Table 3 Comparative analysis of DLNSKNN-DD method with existing models

Methods	$Accu_y$	$Sens_y$	$Spec_y$	F_{score}
DLNSKNN-DD	99.64	95.83	99.28	97.50
SCODL-DDC	99.45	94.65	99.11	97.27
Fusion Model	98.97	92.86	98.45	93.16
InceptionV3	97.65	94.26	97.68	90.43
ResNet50	97.08	88.17	97.85	84.07
VGG16	96.59	86.57	97.80	83.26
AD-TLCNN	95.07	94.46	97.18	92.33
FM-HCF-DLF	94.71	93.59	94.77	93.60

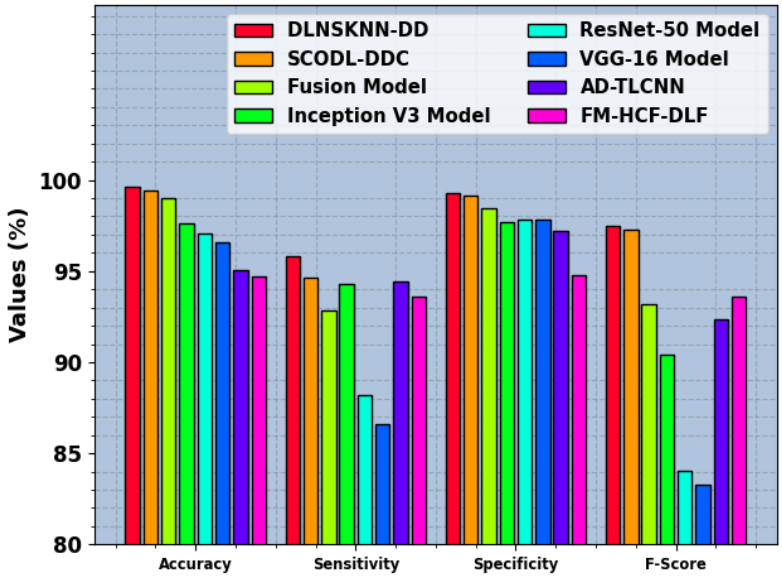

Figure 5: Comparative analysis of DLNSKNN-DD technique with recent models

Thus, the DLNSKNN-DD technique can be applied for enhanced performance compared to recent models.

5. Conclusion

In this study, we have designed a new DLNSKNN-DD method. The objective of the DLNSKNN-DD technique is to detect the presence of virus pneumonia and COVID-19. It contains three distinct kinds of processes selection, optimization, and classification process. In the DLNSKNN-DD technique, the feature extraction from the medical images is carried out by ResNet50v2. Moreover, the parameter tuning of the ResNetv2 model is done using Adadelta optimizer. For classification purposes, the DLNSKNN-DD technique exploits NSKNN model. The performance evaluation of the DLNSKNN-DD method can be assessed on medicinal image dataset. The experimental outcomes underlined the effectual recognition results of the DLNSKNN-DD technique on the identification of diseases

Funding: "This research received no external funding"

Conflicts of Interest: "The authors declare no conflict of interest."

References

[1] Abobala, M., "AH-Subspaces in Neutrosophic Vector Spaces", International Journal of Neutrosophic Science, Vol. 6, pp. 80-86, 2020.

DOI: https://doi.org/10.54216/IJNS.250105
Received: February 01, 2024 Revised: April 02, 2024 Accepted: June 21, 2024

[2] Abobala, M., "A Study of AH-Substructures in n-Refined Neutrosophic Vector Spaces", International Journal of Neutrosophic Science", Vol. 9, pp.74-85, 2020.
[3] Khalid, M., Khalid, N.A. and Iqbal, R., 2020. MBJ-neutrosophic T-ideal on B-algebra. International Journal of Neutrosophic Science, 1(1), pp.29-39.
[4] Gamboa-Cruzado, J., Morante-Palomino, E., Rivero, C.A., Bendezú, M.L. and Fernández, D.M.M., 2024. Research on the Classification and Application of Physical Education Teaching Mode by Neutrosophic Analytic Hierarchy Process. International Journal of Neutrosophic Science, 23(3), pp.51-1.
[5] Mathew, L.P., Sebastian, L. and Thankachan, B., 2024. Some Operations on Trapezoidal Single Valued Neutrosophic Fuzzy Numbers. International Journal of Neutrosophic Science, 23(3), pp.29-9.
[6] Goyal, S. and Singh, R., 2023. Detection and classification of lung diseases for pneumonia and Covid-19 using machine and deep learning techniques. Journal of Ambient Intelligence and Humanized Computing, 14(4), pp.3239-3259.
[7] Sanghvi, H.A., Patel, R.H., Agarwal, A., Gupta, S., Sawhney, V. and Pandya, A.S., 2023. A deep learning approach for classification of COVID and pneumonia using DenseNet-201. International Journal of Imaging Systems and Technology, 33(1), pp.18-38.
[8] Ali, A.M., Ghafoor, K., Mulahuwaish, A. and Maghdid, H., 2024. COVID-19 pneumonia level detection using deep learning algorithm and transfer learning. Evolutionary Intelligence, 17(2), pp.1035-1046.
[9] Mohan, G., Subashini, M.M., Balan, S. and Singh, S., 2024. A multiclass deep learning algorithm for healthy lung, Covid-19 and pneumonia disease detection from chest X-ray images. Discover Artificial Intelligence, 4(1), p.20.
[10] Mehmood, M.H., Hassan, F., Rahman, A.U., Khan, W., Mostafa, S.M., Ghadi, Y.Y., Algarni, A. and Ali, M., 2024. CP_DeepNet: a novel automated system for COVID-19 and pneumonia detection through lung X-rays. Multimedia Tools and Applications, pp.1-18.
[11] Ibrahim, D.M., Elshennawy, N.M. and Sarhan, A.M., 2021. Deep-chest: Multi-classification deep learning model for diagnosing COVID-19, pneumonia, and lung cancer chest diseases. Computers in biology and medicine, 132, p.104348.
[12] Albahli, S. and Nazir, T., 2023. A Circular Box-Based Deep Learning Model for the Identification of Signet Ring Cells from Histopathological Images. Bioengineering, 10(10), p.1147.
[13] Alhasson, H.F., Almozainy, E., Alharbi, M., Almansour, N., Alharbi, S.S. and Khan, R.U., 2023. A Deep Learning-Based Mobile Application for Monkeypox Detection. Applied Sciences, 13(23), p.12589.
[14] Wirtz, A., Mirashi, S.G. and Wesarg, S., 2018. Automatic teeth segmentation in panoramic X-ray images using a coupled shape model in combination with a neural network. In Medical Image Computing and Computer Assisted Intervention–MICCAI 2018: 21st International Conference, Granada, Spain, September 16-20, 2018, Proceedings, Part IV 11 (pp. 712-719). Springer International Publishing.
[15] Almubark, I., Chang, L.C., Shattuck, K.F., Nguyen, T., Turner, R.S. and Jiang, X., 2020. A 5-min cognitive task with deep learning accurately detects early Alzheimer's disease. Frontiers in aging neuroscience, 12, p.603179.
[16] Chatterjee, S., Saad, F., Sarasaen, C., Ghosh, S., Krug, V., Khatun, R., Mishra, R., Desai, N., Radeva, P., Rose, G. and Stober, S., 2024. Exploration of interpretability techniques for deep covid-19 classification using chest x-ray images. Journal of Imaging, 10(2).
[17] Althaqafi, T., Al-Ghamdi, A.S.A.M. and Ragab, M., 2023, April. Artificial intelligence based COVID-19 detection and classification model on chest X-ray images. In Healthcare (Vol. 11, No. 9, p. 1204). MDPI.
[18] Kumar, M., SL, S.D. and Prashanth, B.S., 2024. CXNet-A Novel approach for COVID-19 detection and Classification using Chest X-Ray image. Procedia Computer Science, 235, pp.2486-2497.
[19] Islam, M.K., Rahman, M.M., Ali, M.S., Miah, M.S. and Rahman, M.H., 2023. An Enhanced Technique of COVID-19 Detection and Classification Using Deep Convolutional Neural Network from Chest X-Ray and CT Images. BioMed Research International, 2023(1), p.6341259.
[20] Hilali-Jaghdam, I., Elhag, A.A., Ishak, A.B., Elnaim, B.M.E., Elhag, O.E.M., Abuhaimed, F.M. and Abdel-Khalek, S., 2024. Towards COVID-19 detection and classification using optimal efficient Densenet model on chest X-ray images. Alexandria Engineering Journal, 101, pp.136-146.
[21] Balasubramaniam, S. and Kumar, K.S., 2023. Optimal Ensemble learning model for COVID-19 detection using chest X-ray images. Biomedical Signal Processing and Control, 81, p.104392.
[22] https://github.com/ieee8023/covid-chestxray-dataset
[23] Sharmin, S., Ahammad, T., Talukder, M.A. and Ghose, P., 2023. A hybrid dependable deep feature extraction and ensemble-based machine learning approach for breast cancer detection. IEEE Access
[24] Wang, Z., Yang, M., Jiao, Q., Xu, L., Han, B., Li, Y. and Tan, X., 2024. Two-Level Spatio-Temporal Feature Fused Two-Stream Network for Micro-Expression Recognition. Sensors, 24(5), p.1574
[25] Saqlain, M., Riaz, M., Saleem, M.A. and Yang, M.S., 2021. Distance and similarity measures for neutrosophic hypersoft set (NHSS) with construction of NHSS-TOPSIS and applications. IEEE Access, 9, pp.30803-30816.

DOI: https://doi.org/10.54216/IJNS.250105
Received: February 01, 2024 Revised: April 02, 2024 Accepted: June 21, 2024

[26] Akbulut, Y., Sengur, A., Guo, Y. and Smarandache, F., 2017. NS-k-NN: Neutrosophic set-based k-nearest neighbors classifier. Symmetry, 9(9), p.179.

DOI: https://doi.org/10.54216/IJNS.250105
Received: February 01, 2024 Revised: April 02, 2024 Accepted: June 21, 2024